J Physiol 592.18 (2014) pp 4083–4096

The Journal of Physiology

The impact of ageing on adipose structure, function and vasculature in the B6D2F1 mouse: evidence of significant multisystem dysfunction

Anthony J. Donato[1,2,3], Grant D. Henson[3], Corey R. Hart[3], Gwenael Layec[1], Joel D. Trinity[1], R. Colton Bramwell[1], Ryley A. Enz[1], R. Garrett Morgan[1], Kelly D. Reihl[1], Sugata Hazra[1], Ashley E. Walker[1], Russell S. Richardson[1,2,3] and Lisa A. Lesniewski[1,2,3]

[1] *Division of Geriatrics, Department of Internal Medicine, University of Utah School of Medicine, Salt Lake City, UT, USA*
[2] *Geriatrics Research Education and Clinical Center, Veteran's Affairs Medical Center-Salt Lake City, Salt Lake City, UT, USA*
[3] *Department of Exercise and Sports Science, University of Utah, Salt Lake City, UT, USA*

Key points

- Dysfunction in the adipose tissue, characterized by reduced adipocyte size, tissue fibrosis and ectopic lipid accumulation, has been implicated in age-associated metabolic dysfunction, but it is not known how ageing affects the function of the arteries and mitochondria within the adipose tissue.
- Mitochondrial lipid utilization is impaired in adipose tissue of old mice, evidenced by reduced substrate control ratios in the presence of lipid substrates and is concomitant with increased oxidative stress.
- Ageing leads to endothelial dysfunction, evidenced by reduced endothelium-dependent dilation in resistance arteries, reduced angiogenic capacity and reduced vascularity of the adipose tissue.
- These results indicate that arterial and mitochondrial dysfunction accompany age-associated adipose tissue and systemic metabolic dysfunction and suggest that targeting arterial or mitochondrial function to improve adipose tissue function may have important application in the treatment of age-associated metabolic dysfunction.

Abstract The critical influence of the white adipose tissue (WAT) on metabolism is well-appreciated in obesity, but adipose tissue dysfunction as a mechanism underlying age-associated metabolic dysfunction requires elucidation. To explore this possibility, we assessed metabolism and measures of epididymal (e)WAT mitochondria and artery function in young (6.1 ± 0.4 months) and old (29.6 ± 0.2 months) B6D2F1 mice. There were no group differences in average daily oxygen consumption, fasted blood glucose or plasma free fatty acids, but fasted plasma insulin and the homeostatic model assessment of insulin resistance (HOMA-IR%) were higher in the old (~50–85%, $P < 0.05$). Tissue mass ($P < 0.05$) and adipocyte area were lower (~60%) ($P < 0.01$) and fibrosis was greater (sevenfold, $P < 0.01$) in eWAT with older age. The old also exhibited greater liver triglycerides (~60%, $P < 0.05$). The mitochondrial respiratory oxygen flux after the addition of glutamate and malate (GM), adenosine diphosphate (d), succinate (S) and octanoyl carnitine (O) were one- to twofold higher in eWAT of old mice ($P < 0.05$). Despite no change in the respiratory control ratio, substrate control ratios of GMO_d/GM_d and $GMOS_d/GM_d$ were ~30–40% lower in old mice ($P < 0.05$) and were concomitant with increased nitrotyrosine ($P < 0.05$) and reduced expression of brown adipose markers ($P < 0.05$). Ageing reduced vascularity (~50%, $P < 0.01$), angiogenic capacity (twofold, $P < 0.05$) and expression of vascular endothelial growth factor (~50%, $P < 0.05$) in eWAT. Finally, endothelium-dependent dilation was lower ($P < 0.01$) in isolated arteries from eWAT arteries of the old mice. Thus,

DOI: 10.1113/jphysiol.2014.274175

metabolic dysfunction with advancing age occurs in concert with dysfunction in the adipose tissue characterized by both mitochondrial and arterial dysfunction.

(Received 7 March 2014; accepted after revision 6 July 2014; first published online 18 July 2014)
Corresponding Author: L. A. Lesniewski, Ph.D., Division of Geriatrics, Department of Internal Medicine, University of Utah and VA Medical Center-SLC, GRECC Building 2, Rm 1C06, 500 Foothill Dr., Salt Lake City, UT 84148, USA. Email: lisa.lesniewski@utah.edu

Abbreviations ACh, acetylcholine; *Cidea1*, cell death-inducing DFFA-like effector a; EDD, endothelium-dependent dilation; Elovl3, fatty acid elongase 3; eWAT, epididymal white adipose tissue; GM, glutamate and malate; HOMA-B%, homeostatic model assessment of β cell function; HOMA-IR%, homeostatic model assessment of insulin resistance; IC_{50}, sensitivity; J_{O_2}, mitochondrial respiratory oxygen flux; L-NAME, N^G-nitro-L-arginine methyl ester; NO, nitric oxide; PECAM-1, platelet endothelial cell adhesion molecule 1; ROS, reactive oxygen species; *Ucp1*, uncoupling protein 1; VEGF, vascular endothelial growth factor.

Introduction

Ageing is an independent risk factor for the development of insulin resistance (Jackson *et al.* 1988; Karakelides *et al.* 2010), with older adults of normal weight (55–64 years) demonstrating the same relative risk of diabetes as younger patients with a body mass index (BMI) greater than 30 kg m^{-2} (Lindstrom & Tuomilehto, 2003). While the role of the skeletal muscle and liver in the development of insulin resistance and type 2 diabetes is well known, the adipose tissue has only recently become recognized as an important factor in metabolic homeostasis. No longer thought to be an inert energy storage site, the adipose tissue is now known to be a metabolically active endocrine organ (Frayn, 2002) that plays a critical role in maintaining metabolic homeostasis (Goossens, 2008). Conditions characterized by gross alterations in the capacity for normal lipid storage, whether increased storage as in obesity or decreased storage as in lipodystrophy, result in systemic metabolic derangements (Garg, 2006). Dysfunction of the adipose tissue in these states of altered lipid storage is implicated in this systemic dysfunction (Garg, 2006).

In obesity, adipose tissue dysfunction is often characterized by enlarged adipocytes, adipose tissue inflammation and fibrosis, ectopic lipid accumulation and hyperlipidaemia (Frayn, 2002; Trayhurn & Wood, 2004; Lesniewski *et al.* 2007; Goossens, 2008; Lumeng *et al.* 2008; Divoux *et al.* 2010; Sun *et al.* 2011). Unlike obesity, advanced age is associated with a reduction in adipose mass (Chumlea *et al.* 1989; Kirkland *et al.* 2002) that may result from an increased presence of small dysfunctional 'mesenchymal adipocyte-like' cells (Kirkland *et al.* 1994; Kirkland & Dobson, 1997) with a reduced capacity for lipid accumulation that contributes to a redistribution of lipid stores outside of the appropriate adipose storage sites (Kirkland *et al.* 2002). However, at the same time, ageing is associated with other aspects of adipose tissue dysfunction that are commonly associated with obesity such as an increase in the ectopic storage of lipids (Kirkland *et al.* 2002), inflammation (Wu *et al.* 2007), as well as tissue hypoxia and oxidative stress (Zhang *et al.* 2011). These features could also be associated with mitochondrial dysfunction and increased mitochondrial derived reactive oxygen species (ROS) production in adipose tissue. Indeed, in skeletal muscle, old mice have greater mitochondrial-derived ROS compared to young mice (Mansouri *et al.* 2006), but mitochondrial function and ROS production in the adipose tissue with ageing has not been studied.

Adequate perfusion is required to maintain adipose tissue homeostasis and therefore the vascular endothelium of the adipose arteries plays a critical role in maintaining tissue perfusion by contributing to both vasodilation and the initiation of the angiogenic processes. We have recently demonstrated that a high fat diet impairs endothelium-dependent dilation (EDD) and reduces the bioavailability of nitric oxide (NO) in adipose tissue arteries from young mice (Donato *et al.* 2012) and this endothelial dysfunction was associated with metabolic derangements and adipose tissue inflammation. Likewise, angiogenic capacity is impaired in subcutaneous adipose tissue from obese patients (Gealekman *et al.* 2011). However, it is not known if ageing induces a similar impairment in EDD or angiogenic capacity in the adipose resistance arteries as observed with obesity/high fat diet. With ageing, alterations in adipose tissue vascularity, impairments in angiogenic capacity and arterial reactivity may lead to inadequate perfusion of the adipose tissue and subsequent adipose dysfunction.

We hypothesized that age-related impairments in metabolic homeostasis would be associated with adipose tissue dysfunction characterized by increased mitochondrial ROS production, reduced vascularity, impaired angiogenic capacity and impaired resistance artery endothelial dysfunction as a consequence of reduced NO bioavailability. To test these hypotheses, we utilized a well-established model of arterial ageing (Reddy *et al.* 2003; Lesniewski *et al.* 2009) to assess adipose tissue

metabolic, mitochondrial and arterial function in young and old mice.

Methods

Ethical approval

All animal procedures conformed to the *Guide to the Care and Use of Laboratory Animals* (National Research Council (U.S.). Committee for the Update of the Guide for the Care and Use of Laboratory Animals. *et al.*, 2011) and were approved by the University of Utah and Salt Lake City VA Medical Center Animal Care and Use Committee.

Animals

Young (6.1 ± 0.4 months) male B6D2F1 mice ($n = 35$) were obtained from Charles River Inc. and old (29.6 ± 0.2 months) male mice ($n = 28$) were purchased from the ageing colonies maintained at Charles River Inc. (Wilmiington, MA) for the National Institute on Aging. All mice were housed in standard mouse cages in an animal care facility at the Veterans Affairs Medical Center-Salt Lake City on a 12:12 light/dark cycle and provided normal rodent chow (8640 Harlan Teklad 22/5 Standard Rodent Chow) and water ad libitum. Animals were killed for tissue harvest in the morning in the fed state. Before tissue harvest, animals were weighed and a blood glucose measurement was made via tail nick. Mice were killed by exsanguination via cardiac puncture while they were maintained under anaesthesia by inhaled isoflurane. Blood collected at death was used for measures of fed plasma free fatty acid concentrations (Donato *et al.* 2012).

Metabolic assessment

A subset of mice ($n = 5$/group) were housed in metabolic cages for 3 nights/2 days to assess oxygen consumption, respiratory exchange ratio, food and water intake as well as spontaneous cage activity. In addition, intraperitoneal glucose tolerance tests were performed (2 g kg^{-1}, I.P.) and insulin resistance and β cell function were estimated from fasted blood glucose and plasma insulin using the Homeostatic Model Assessment (HOMA) (Turner *et al.* 1979; Donato *et al.* 2012). Glucose tolerance tests and collection of blood glucose and plasma for HOMA calculations were performed after a 2 h morning fast. Although the HOMA parameters can be approximated using simple linear equations yielding estimates of insulin resistance (IR) and β cell function (B), an updated more appropriate non-linear model (HOMA2) was described by Levy *et al.* (1998) and a computer-based calculator program is available online (http://www.dtu.ox.ac.uk/homacalculator/index.php). This calculator was used to determine HOMA-IR% and HOMA-B% from the same fasted blood sample. Plasma collected from this fasted blood sample as well as in the fed state at death was also used to determine non-esterified free fatty acid concentrations (NEFA kit; Wako, Richmond, VA).

Adipocyte morphology, adipose fibrosis and tissue volumes

One epididymal white adipose tissue (eWAT) pad from each animal was weighed, fixed overnight in 10% formalin and embedded in paraffin for histological sectioning. Ten micron sections were cut on a microtome and stained with haematoxylin and eosin for measures of adipocyte cross-sectional area or with picrosirius red to identify collagen, an assessment of tissue fibrosis. For cross-sectional area measures, an average of 521 ± 71 cells per animal were measured with a range of 211–800 cells per animal. Cell areas were averaged to obtain mean cross-sectional area and were binned by area to examine the distribution of cell sizes within the sections. Analyses of both morphology and fibrosis were performed using ImageJ software (NIH freeware). The number of adipocytes measured per animal was not the same for all animals due to the size of the fat pad and differences in the number of adipocytes present in a given histological section. Measurements were made in all adipocytes with an intact membrane in the visual field for images collected using a ×20 objective. All images were collected on the same microscope. For tissue slices that were too large to visualize in their entirety within a single image, four images were collected from distinct areas distributed throughout the fat pad. Computed tomography (CT) scans were performed on an additional group of young (8 months, $n = 5$) and old (25 months, $n = 4$) male mice to assess entopic adipose tissue volumes in the visceral and subcutaneous depots. Micro-CT data were collected in anaesthetized mice (2–5% isoflurane/O_2 gas) utilizing a Quantum FX Micro CT Scanner (Perkin-Elmer, Waltham, MA). Voltage was set at 50 kV and current was set at 200 μA and the images were captured over a 4.5 min interval. The abdominal region was defined superiorly by the diaphragm and inferiorly by the pelvic epiphysis. Analysis was conducted with Caliper Analyze 11.0 (Analyze Direct, Overland Park, KS). Visceral and subcutaneous adipose tissue was segmented in the sagittal plane and volume measurements obtained with the Region of Interest module. Tissue volumes are expressed relative to body mass.

Liver and skeletal muscle lipid accumulation

The liver and quadriceps muscles were excised and weighed. Lipid was extracted from approximately 100 mg of tissue as described previously (Lindstrom & Tuomilehto, 2003; Rodriguez-Sureda & Peinado-Onsurbe,

2005). Triglyceride content was assessed using a commercially available assay kit (Cayman Chemicals, Ann Arbor, MI) and expressed as a percentage of starting tissue mass.

Mitochondrial function

All tissue was stored and transferred in precooled buffer A (in mM: 10 Ca^{2+}/EGTA buffer, 20 imidazole, 50 K^+/4-morpholinoethanesulfonic acid, 0.5 dithiothreitol, 6.56 $MgCl_2$, 5.77 ATP, 15 phosphocreatine, pH 7.1) less than 30 min before respiration measurements. The tissue was dissected under magnification on ice with forceps to carefully remove blood vessels and connective tissue. The tissue was then rinsed twice in buffer B (in mM: 2.77 CaK_2EGTA, 7.23 K_2EGTA, 1.38 $MgCl_2$, 3.0 K_2HPO_4, 0.5 dithiothreitol, 20 imidazole, 100 K-MES, 20 taurine, pH 7.3 at 4°C) for 10 min and permeabilized with digitonin (2 μM) in the 2 ml respiratory chamber (Kraunsoe *et al.* 2010).

Mitochondrial respiratory oxygen flux (J_{O_2}) was assessed with a Clark type, high resolution respirometer (Hansatech, Norfolk, UK). Tissue (~2–3 mg muscle; ~50 mg epididymal adipose tissue) was studied in duplicate and incubated in the respirometer with 2 ml of buffer B and stirred continuously at 37°C. First, baseline respiration was recorded without addition of mitochondrial respiration substrates. To measure complex-specific oxygen consumption, respiratory substrates were applied in the following order (final concentrations in 2 ml chamber): glutamate–malate (GM, both 10 mM), ADP (GM_d, 5 mM), octanoyl carnitine (GMO_d, 1.5 mM) and succinate ($GMOS_d$, 10 mM). Finally, cytochrome *c* (10 μM) was added to test the integrity of the outer mitochondrial membrane. The respiration rates were recorded for 5 min at each stage, and the average of the final minute was used for the data analysis. Rates of O_2 consumption were expressed in pmol O_2 per second per milligram wet weight. Control ratios, including the respiratory control ratio, and substrate control ratio, were calculated from the respiratory flux measurements as described previously (Kraunsoe *et al.* 2010). Following the respiration measurements, the tissue samples were frozen in liquid nitrogen and stored at −80°C for further mitochondrial DNA analysis.

Adipose tissue oxidative stress

Nitrotyrosine abundance, a marker of tissue oxidative stress, was assessed in adipose tissue lysates by standard Western blot procedures using a primary antibody against nitrotyrosine (Abcam; Cambridge, MA, ab 110282, 1:200) and β-actin (Ab 8227, 1:500) to normalize for protein loading. Proteins were visualized by chemiluminescence, imaged with a BioRad (Hercules, CA) Molecular Imager with ImageLab software and quantified using ImageJ software (NIH freeware).

Brown adipose tissue markers

As decreases in beige adipose, i.e. brown-like adipocytes within white adipose depots, are associated with metabolic disease (Rogers *et al.* 2012; Harms & Seale, 2013) and have been observed in the subcutaneous WAT of mice with advancing age (Rogers *et al.* 2012), total RNA was isolated from eWAT and cDNA was prepared per manufacturer's instructions. Gene expression for the brown adipose tissue markers uncoupling protein 1 (*Ucp1*) (primer sequences: forward: ACT GCC ACA CCT CCA GTC ATT; reverse: CTT TGC CTC ACT CAG GAT TGG), cell death-inducing DFFA-like effector a (*Cidea1*) (primer sequences: forward: TGC TCT TCT GTA TCG CCC AGT; reverse: GCC GTG TTA AGG AAT CTG CTG) and fatty acid elongase 3 (*Elovl3*) (primer sequences: forward: TCC GCG TTC TCA TGT AGG TCT; reverse: GGA CCT GAT GCA ACC CTA TGA), were determined by polymerase chain reaction (PCR). RNA quantification was performed with the BioRad iQ5 Realtime PCR machine.

Adipose tissue vascularity

Vascular structures in adipose were identified on 8 μm paraffin-embedded sections using a platelet/endothelial cell adhesion molecule-1 (PECAM-1 or CD31) antibody. Tissue was incubated with anti-PECAM-1 (no. ab28364; Abcam) overnight, and then stained with Tyramide Signal Amplification (no. T-20926; Life Technologies). Epifluorescent images were captured using BD Pathway 855 with a ×10 objective. Image analysis was conducted using ImageJ software (NIH freeware). Only vascular structures between 6.5 and 240 μm (8–300 pixels) were counted in the analysis. Vascular density was then normalized to total nuclei count, visualized using Hoechst 33342 staining (no. H3570; Life Technologies).

Angiogenic capacity

The angiogenic capacity of the adipose tissue was assessed by quantifying sprout formation *in vitro* as described previously (Gealekman *et al.* 2011). Briefly, a small (1 mm^2) explant of the eWAT was embedded in a collagen matrix and cultured in standard medium supplemented with vascular endothelial growth factor (VEGF: 0.5 mg ml^{-1}). Growth medium changes were performed every other day. Five days after explantation, sprouts were assessed by visualizing cultures with phase contrast on an inverted microscope (Nikon Instruments, Melville, NY).

Adipose *Vegf* gene expression

Total RNA was isolated from eWAT and gene expression for *Vegf* was determined by PCR (primer sequences: forward: CCT GGT GGA CAT CTT CCA GGA GTA CC; reverse: GAA GCT CAT CTC TCC TAT GTG CTG GC). RNA quantification was performed with the BioRad iQ5 Realtime PCR machine (Life Technologies).

Endothelial function

To assess endothelial function, arteries were excised, cleared of surrounding adipose tissue and cannulated on the stage of a pressure myograph (DMT Inc., Atlanta, GA, USA). Arteries were pre-constricted with 2 μM phenylephrine and EDD as well as the contribution of NO to dilation were measured in response to the cumulative addition of acetylcholine (ACh: 1×10^{-9} to 1×10^{-4} mol l^{-1}) in the absence or presence of the NO synthase inhibitor, N^G-nitro-L-arginine methyl ester (L-NAME: 0.1 mmol l^{-1}, 30 min), as described previously (Lesniewski *et al.* 2009). Endothelium-independent dilation was assessed in response to sodium nitroprusside (1×10^{-10} to 1×10^{-4} mol l^{-1}) (Lesniewski *et al.* 2009). After completion of dose–responses, vessels were incubated (≥60 min) in a calcium-free physiological salt solution and maximal artery diameter measured. Vessel diameters were measured by MyoView software (DMT Inc.). All dose–response data are presented as a percentage of possible dilation after pre-constriction to phenylephrine. Arteries failing to achieve ≥20% pre-constriction were excluded. Sensitivity was defined as the concentration of ACh or sodium nitroprusside that elicited 50% of the maximal response (IC_{50}). Sensitivities were calculated using BioDataFit 1.02. A regression was used to fit a sigmoidal model to individual dose–responses yielding a dose for the half maximal response in log M units.

Statistics

To determine required group sizes, power analyses were performed on published and preliminary data for primary outcome measures using G*Power. Before assessing group differences, normality was determined by the Shapiro–Wilks test for normality ($P > 0.05$). Group differences for dose–responses to ACh or sodium nitroprusside and adipocyte area distribution analyses were determined by repeated measures analysis of variance (ANOVA). All other group differences were determined by Student's *t* tests. Data are presented as means ± S.E.M. Significance was set at $P < 0.05$.

Table 1. Age, body and tissue masses of young and old B6D2F1 mice

	Young	Old
n	9	9
Age (months)	6.1 ± 0.4	29.6 ± 0.2*
BM (g)	37.9 ± 1.5	35.4 ± 0.8
WAT mass (g)	0.7 ± 0.1	0.4 ± 0.1*
WAT/BM (%)	*1.8 ± 0.2*	*1.2 ± 0.4*
Gast (g)	0.18 ± 0.01	0.13 ± 0.01*
Gast/BM (%)	*0.49 ± 0.03*	*0.38 ± 0.03**
Heart mass (g)	0.17 ± 0.01	0.21 ± 0.01*
Heart/BM (%)	*0.45 ± 0.02*	*0.57 ± 0.03**
Liver (g)	1.7 ± 0.1	2.0 ± 0.1*
Liver/BM (%)	*4.6 ± 0.2*	*5.9 ± 0.2**

$P \leq 0.05$, means ± S.E.M. Abbreviations: BM, body mass; Gast, gastrocnemius muscle mass; WAT, white adipose tissue. *Denotes difference from young.

Results

Body and tissue masses

Total body mass did not differ between young ($n = 9$) and old ($n = 9$) B6D2F1 mice (Table 1). Advancing age was associated with a ∼40% reduction ($P < 0.05$) in absolute eWAT mass (Table 1). Absolute gastrocnemius muscle mass ($P < 0.01$) and gastrocnemius muscle mass relative to body mass ($P < 0.05$) was lower in old compared to young mice (Table 1). Absolute heart mass ($P < 0.05$) and heart mass relative to body mass ($P = 0.01$) was higher in old mice (Table 1). Absolute liver mass was higher in old mice compared to young ($P < 0.01$) and remained higher ($P < 0.01$) when expressed relative to body mass (Table 1).

Metabolic assessment

Average daily oxygen uptake ($\dot{V}_{O_2}$: 2780 ± 91 *vs.* 2547 ± 139 ml kg^{-1} h^{-1}) and carbon dioxide production ($\dot{V}_{CO_2}$: 2318 ± 54 *vs.* 2220 ± 138 ml kg^{-1} h^{-1}) did not differ between young ($n = 5$) and old ($n = 5$) mice, although the respiratory exchange ratio (0.83 ± 0.01 *vs.* 0.86 ± 0.01, $P = 0.09$) tended to be higher in the old mice. Heat production (0.52 ± 0.02 *vs.* 0.46 ± 0.04 kcal h^{-1}) was not different between groups. Food intake was higher (6.0 ± 0.4 *vs.* 7.9 ± 0.6 g, $P < 0.05$) and water intake (4.8 ± 0.5 *vs.* 7.9 ± 1.4 g, $P = 0.06$) tended to be higher in old *versus* young mice. There were no differences in spontaneous cage activity (972 ± 90 *vs.* 817 ± 83 beam breaks day^{-1}) between young and old mice. Note that Table 2 includes metabolic cage data separated into night and day cycles and represents $n = 5$/group.

Although fasted blood glucose did not differ between age groups, fasted plasma insulin was higher ($P = 0.05$)

Table 2. Metabolic and activity measures in young and old B6D2F1 mice (n = 5–13/group)

		Young	Old
Body mass (g)		38.0 ± 1.0	36.2 ± 1.2
$\dot{V}_{O_2}$ (ml kg^{-1} h^{-1})	Night	2797 ± 96	2685 ± 58
	Day	2766 ± 96	2408 ± 145
$\dot{V}_{CO_2}$ (ml kg^{-1} h^{-1})	Night	2346 ± 58	2352 ± 185
	Day	2295 ± 79	2086 ± 152
RER	Night	0.84 ± 0.02	0.87 ± 0.01
	Day	0.83 ± 0.02	0.86 ± 0.02
Heat (kcal h^{-1})	Night	0.52 ± 0.02	0.48 ± 0.04
	Day	0.51 ± 0.02	0.43 ± 0.04
Food intake (g day^{-1})	Night	5.4 ± 0.3	7.3 ± 0.6*
	Day	6.5 ± 0.4	8.9 ± 0.8
Water intake (ml day^{-1})	Night	4.4 ± 0.5	7.4 ± 1.2*
	Day	5.2 ± 0.4	9.2 ± 2.4
Activity (beam breaks day^{-1})	Night	1041 ± 196	976 ± 139
	Day	907 ± 156	651 ± 256
Fasted blood glucose (mg dl^{-1})		124 ± 3	120 ± 4
Fasted plasma insulin (ng ml^{-1})		1.3 ± 0.1	2.4 ± 0.4*
HOMA-IR%		4.6 ± 0.4	7.1 ± 0.3*
HOMA-B%		117 ± 8	184 ± 26*
AUC-GTT (mg dl^{-1} min^{-1})		12557 ± 316	14956 ± 1033*
Plasma FFA (μmol)	Fasted	312 ± 33	347 ± 58
	Fed	726 ± 59	967 ± 150

$P < 0.05$, means ± S.E.M. Abbreviations: AUC-GTT, area under the curve for glucose during glucose tolerance test; FFA, free fatty acids; HOMA-B%, homeostatic model assessment of beta cell function; HOMA-IR%, homeostatic model assessment of insulin resistance; RER, respiratory exchange ratio; $\dot{V}_{CO_2}$, carbon dioxide production; $\dot{V}_{O_2}$, oxygen consumption. *Denotes difference from young.

in old ($n = 5$) compared to young mice ($n = 5$) (Table 2). Old age was associated with an increased HOMA-IR% ($P < 0.01$, $n = 5$/group) and an increased HOMA-B% ($P < 0.05$, $n = 5$/group) (Table 2). Similarly, the area under the curve for glucose during an intraperitoneal glucose tolerance test was higher in old compared to young mice ($n = 5$/group) (Table 2). Plasma free fatty acids were higher, but not statistically different, in either the fasted ($n = 6$/group) or fed ($n = 13$/group) state in old compared to young mice (Table 2).

Adipose tissue morphology, fibrosis and volume

Ageing was associated with a leftward shift in the adipocyte area histogram, with approximately 70% of all adipocytes from the eWAT of the old mice falling into the two smallest adipocyte area bins compared to only approximately 10–15% of the adipocytes from young samples observed in these smallest areas (Fig. 1*A*). This is reflected in a reduction in the mean adipocyte area ($P = 0.01$, Fig. 1*B*) with advancing age ($n = 7$–8/group). There was increased eWAT fibrosis in old mice ($P < 0.01$, Fig. 1*C*), assessed in histological sections by picrosirius red staining for collagen ($n = 6$–8/group). Absolute adipose tissue volume in the visceral and subcutaneous depots (not shown) was lower in old compared to young mice (both $P < 0.05$). Adipose tissue volume expressed relative to body mass (body mass: young: 43 ± 1 g *vs.* old: 39 ± 2 g, $P < 0.05$) in the visceral and subcutaneous depots were also lower in old (25 months of age, $n = 4$) compared to young mice (8 months of age, $n = 5$) (Fig. 1*D*, both $P < 0.05$).

Ectopic lipid accumulation

Liver triglyceride content was higher in old ($n = 8$) compared to young mice ($n = 7$) ($P < 0.01$, Fig. 2*A*). Conversely, ageing did not affect triglyceride content of the quadriceps muscle (Fig. 2*B*, $n = 8$–9/group).

Mitochondrial function, oxidative stress and beige adipose in the epididymal white adipose tissue

Mitochondrial DNA (Fig. 3*A*), a marker of mitochondrial content, did not differ in the eWAT from young ($n = 12$) and old mice ($n = 6$). The mitochondrial respiratory oxygen flux ($n = 6$–12/group) after the addition of GM (young: 0.8 ± 0.1; old: 2.5 ± 1.0 pmol s^{-1} mg^{-1}), adenosine diphosphate (d) (young: 0.8 ± 0.1; old: 2.2 ± 0.5 pmol s^{-1} mg^{-1}), and octanoyl carnitine (O) (young: 1.3 ± 0.2; old: 2.6 ± 0.6 pmol s^{-1} mg^{-1}) were higher in old compared to young mice (all $P < 0.05$). Although the adipose tissue mitochondrial respiratory

control ratio (GM_d/GM) did not differ between young and old mice, the substrate control ratios for octanoyl carnitine with GM (GMO_d/GM_d, $P < 0.05$) and succinate ($GMSO_d/GM_d$, $P = 0.05$) were lower in old compared to young mice (Fig. 3*B*). There was increased nitrotyrosine abundance (Fig. 3*C*, $P < 0.05$), a marker of tissue oxidative stress, in eWAT from old ($n = 5$) compared to young mice ($n = 5$). There was also lower gene expression of the brown adipose markers, *Ucp1*, *Cidea1* and *Elovl3* in the eWAT of old ($n = 7$) compared to young mice ($n = 11$) (Fig. 3*D*, all $P < 0.05$).

Adipose tissue vascularity, angiogenic capacity and gene expression

Vascularity of the eWAT (n = 8–9/group), assessed by counting the number of size-selected vascular structures (determined by PECAM-1 staining) per total nuclei in a histological section, was reduced with ageing ($P < 0.01$, Fig. 4*A*). To assess angiogenic capacity of the eWAT, an *in vitro* sprouting assay was performed and quantified by determining the number of tubes that grow from a collagen embedded eWAT explant. *In vitro* angiogenic sprouting was lower ($P < 0.05$) in adipose tissue explants from old ($n = 6$) compared to young mice ($n = 5$) (Fig. 4*B*) and this was associated with lower gene expression of the pro-angiogenic growth factor, *Vegf*, in the adipose tissue of old ($n = 7$) compared to young mice ($n = 8$) ($P < 0.05$, Fig. 4*C*).

Adipose resistance artery endothelial function

Maximal diameter of the eWAT resistance arteries did not differ between groups (Table 3). EDD of the adipose resistance arteries to ACh (n = 8–9/group) was impaired in old mice ($P < 0.01$, Fig. 5*A*). This difference in the dose–response curve was reflected in a reduced maximal vasodilation and a reduced sensitivity (IC_{50}) to ACh (both

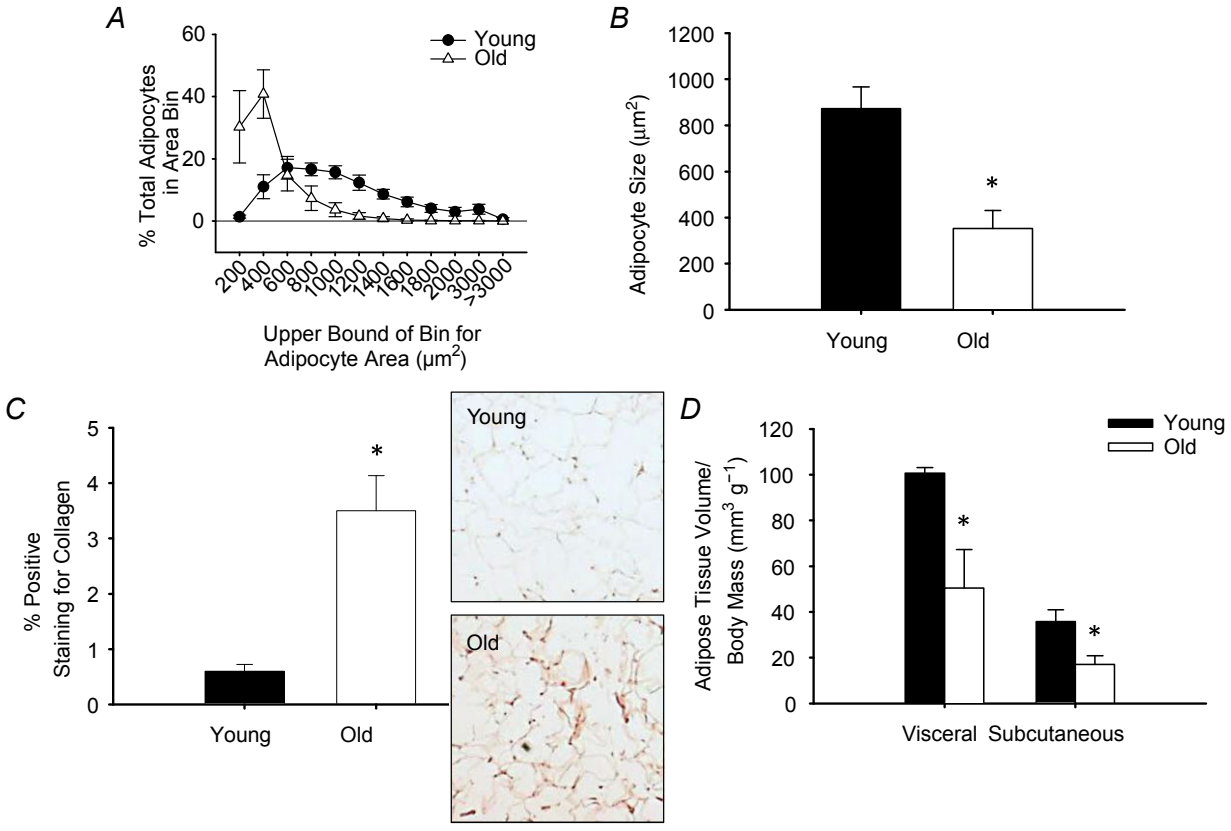

Figure 1. Epididymal white adipose tissue (eWAT) adipocyte area, tissue fibrosis and adipose tissue volumes in young and old mice
Adipocyte area was determined by measuring cross-sectional area of adipocytes (521 ± 71 adipocytes per animal; range: 211–800) on haematoxylin and eosin stained histological sections of eWAT from young (n = 8) and old (n = 7) mice and are presented as a histogram of adipocyte area bins (*A*) and as mean area (*B*). *C*, fibrosis was assessed by picrosirius red staining for collagen in histological sections of eWAT from young (n = 6) and old (n = 8) mice. Representative images shown to the right of the summary data. *D*, visceral and subcutaneous adipose tissue volume was assessed in young (8 months, n = 5) and old (25 months, n = 4) mice by CT and expressed relative to total body mass. *Denotes group difference from young. Data are means ± S.E.M., $P \leq 0.05$.

$P < 0.05$) in old compared to young mice (Table 3). Pre-constriction to phenylephrine did not differ between young and old mice (Table 3).

Inhibition of NO synthase by L-NAME reduced the dose–response ($P < 0.01$) and maximal dilation (both $P < 0.01$) to ACh in both young ($n = 8$) and old mice ($n = 9$), eliminating differences observed in the dose–response ($P = 0.66$, Fig. 5*A*), maximal dilation ($P = 0.3$, Table 3) and sensitivity ($P = 0.83$, Table 3) to ACh alone, indicative of impaired NO bioavailability. L-NAME

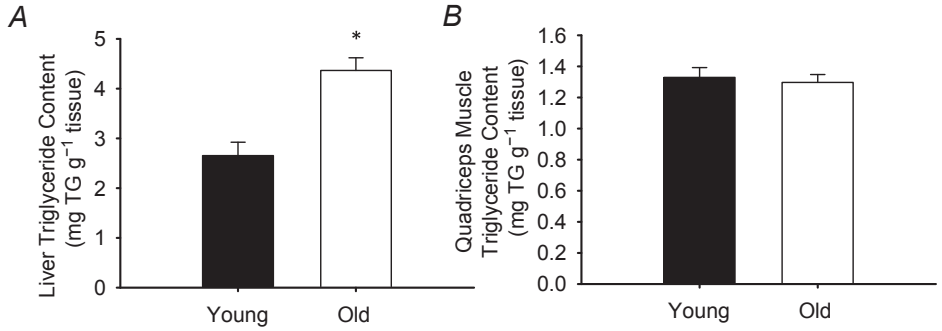

Figure 2. Ectopic lipid accumulation in young and old mice
Ectopic lipid accumulation was assessed by measuring triglyceride content of the liver (*A*) and quadriceps muscle (*B*) in young ($n = 7$–8) and old ($n = 8$–9) mice. *Denotes group difference from young. Data are means ± S.E.M., $P \leq 0.05$.

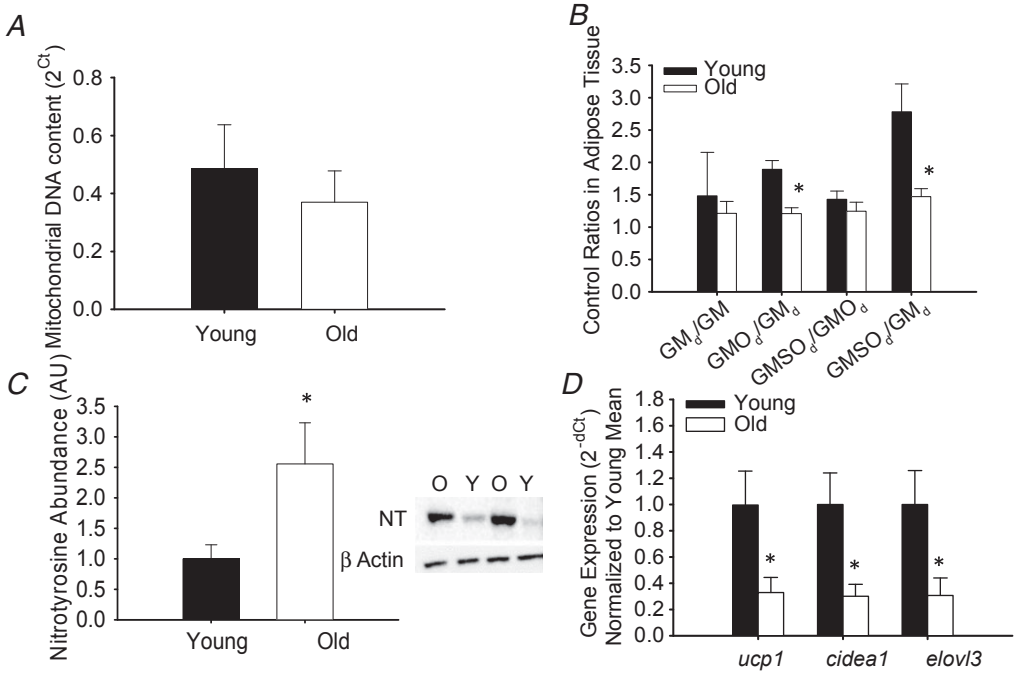

Figure 3. Mitochondrial DNA content, respiratory and substrate control ratios in the epididymal white adipose tissue (eWAT) as well as brown adipose tissue marker expression within eWAT from young and old mice
A, mitochondrial DNA was assessed as a marker of mitochondrial density in the eWAT from young and old mice. *B*, mitochondrial control ratios in eWAT from young and old mice. Respiratory control ratio calculated as GM_d/GM (state 3/state 2 respiration). Substrate control ratios were assessed to determine the relative control exerted by a given substrate on respiration, calculated as the effect of octanoyl carnitine (GMO_d/GM_d), the effect of succinate ($GMSO_d/GMO_d$) and the effect of both octanoyl carnitine and succinate ($GMSO_d/GM_d$). *C*, nitrotyrosine abundance, a marker of tissue oxidative stress, was assessed by Western blot in adipose tissue lysates from young ($n = 5$) and old ($n = 5$) mice. Representative blot images for nitrotyrosine and beta actin are provided to the right of the summary data (Y: young, O: old). *D*, beige fat in the eWAT was determined by assessing uncoupling protein 1 (*Ucp1*), cell death-inducing DFFA-like effector a (*Cidea1*) and fatty acid elongase 3 (*Elovl3*) gene expression in the eWAT of young ($n = 11$) and old ($n = 7$) mice. *Denotes group difference from young. Data are means ± S.E.M., $P \leq 0.05$.

increased pre-constriction in the young mice ($P < 0.05$) and tended to increase pre-constriction in the old ($P = 0.07$) mice. However, after L-NAME, pre-constriction to phenylephrine remained similar between the young and old mice (Table 3). Endothelium independent dilation to sodium nitroprusside did not differ between groups (Fig. 5*B*, $n = 5$–7/group).

Discussion

The novel findings of the present study are that older age is associated with adipose tissue dysfunction characterized by ectopic (hepatic) lipid accumulation and adipose tissue fibrosis as well as increased adipose mitochondrial oxygen flux, altered lipid utilization, increased tissue oxidative stress and lower gene expression of beige adipose markers in the eWAT, a visceral adipose tissue. This adipose dysfunction was concomitant with vascular dysfunction of the adipose tissue such that there was a reduced vascularity, reduced angiogenic capacity, impaired EDD and reduced NO bioavailability in adipose tissue resistance arteries. These vascular and mitochondrial defects probably contribute to the pro-oxidative adipose tissue phenotype that can further impair both insulin action and vascular function, contributing to systemic metabolic dysfunction and predisposing older adults to a range of chronic diseases.

Adipocyte size, adipose depot volume, ectopic lipids and adipose tissue fibrosis with age

Although adipose dysfunction has been well-described in obesity-associated metabolic dysfunction, the role of adipose dysfunction in age-associated metabolic dysfunction is not well characterized. Reduced adipocyte size and increased ectopic lipid accumulation with ageing have been associated with an impaired capacity for pre-adipocyte differentiation to mature adipocytes as well as increased tumour necrosis factor-alpha release from adipocytes (Kirkland *et al.* 2002). Here, we demonstrate reduced visceral and subcutaneous adipose volumes, as well as reduced adipocyte size with ageing. We also demonstrate increased intrahepatic, but not intramuscular lipids with ageing in the B6D2F1 mouse. The

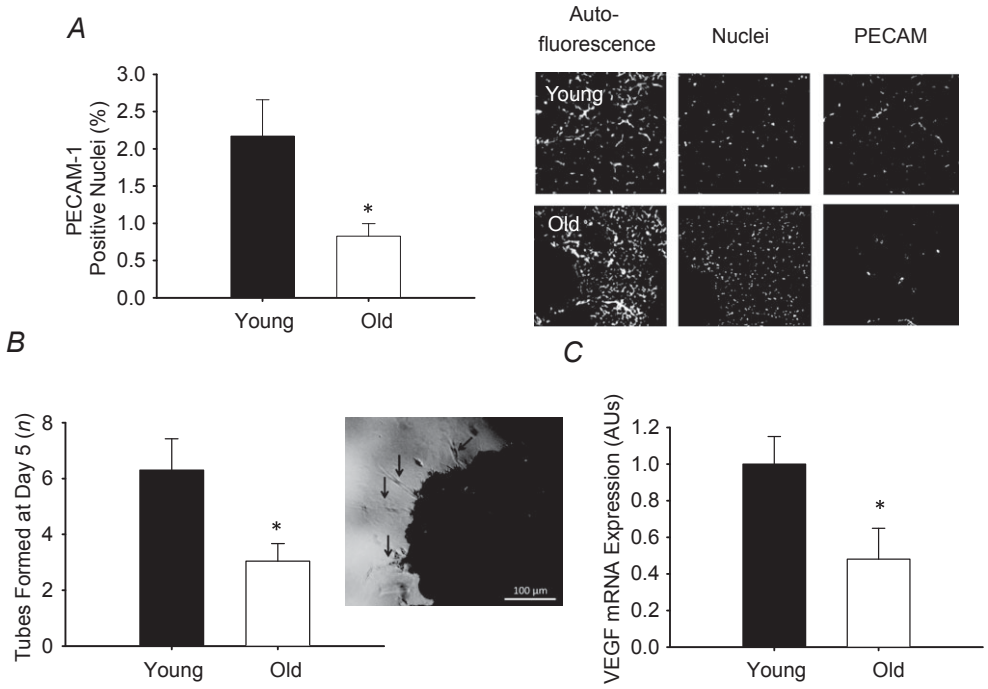

Figure 4. Vascular density, angiogenic capacity and vascular endothelial growth factor expression in the eWAT of young and old mice
A, vascular structures in the eWAT were visualized by immunofluorescent staining using PECAM-1 in young ($n = 8$) and old ($n = 9$) mice. Vascular density is expressed as a percentage of total nuclei. Representative images are provided to the right of the summary graph with adipose autofluorescent panels showing adipocyte morphology. *B*, angiogenic capacity assessed by counting the number of tubes formed in response to stimulation by VEGF (0.5 mg ml^{-1}) by eWAT explants from young ($n = 5$) and old ($n = 6$) mice. A representative image is provided to the right of the summary data. Black arrows indicate tubes sprouting from the tissue explant. *C*, VEGF expression in eWAT from young ($n = 8$) and old ($n = 7$) mice. Data are presented normalized to mean f young mice. *Denotes group difference from young. Data are means ± S.E.M., $P \leq 0.05$. eWAT, epididymal white adipose tissue; PECAM, platelet endothelial cell adhesion molecule; VEGF, vascular endothelial growth factor.

Table 3. Characteristics of isolated resistance arteries excised from the epididymal white adipose tissue of young and old B6D2F1 mice

	Young	Old
n	8	7
Lumen diameter (μm)	207 ± 12	182 ± 19
	ACh	
Pre-constriction (%)	36 ± 6	28 ± 4
Max dilation (%)	97 ± 1	75 ± 12*
EC_{50} [log M]	−8.0 ± 0.4	−6.5 ± 0.4*
	ACh + L-NAME	
Pre-constriction (%)	59 ± 6†	47 ± 11
Max dilation (%)	26 ± 4†	15 ± 4†
EC_{50} [log M]	−7.1 ± 0.2	−7.0 ± 0.7

$P < 0.05$, means ± S.E.M. Abbreviations: ACh, acetylcholine; EC_{50}, sensitivity assessed by determining the dose ACh eliciting half of the maximal dilator response; L-NAME, N^G-nitro-L-arginine methyl ester. *Denotes difference from young. †Denotes difference from ACh alone.

lack of change in intramuscular lipids was contrary to our hypothesis and previous reports in both humans (Kelley *et al.* 1999; Goodpaster *et al.* 2001; Cree *et al.* 2004; Eckel *et al.* 2005) and middle-aged mice (Koonen *et al.* 2010), although the reason for this discrepancy with previously reported findings is unclear, it may be a function of species/strain or age differences. We also provide the first evidence for an increase in adipose tissue fibrosis with ageing. Increased fibrosis is a hallmark of metabolically stressed adipose tissue in obesity and is believed to limit the lipid storage capacity of adipocytes contributing to the redistribution of lipids to ectopic locations (Khan *et al.* 2009). Thus, this age-associated increase in visceral WAT fibrosis may contribute to the observed increase in hepatic lipid accumulation and subsequent systemic dysfunction.

Mitochondrial function

Here, we provide evidence that ageing does not impact visceral WAT mitochondrial density, as assessed by mitochondrial DNA content (Kraunsoe *et al.* 2010) or the mitochondrial respiratory control ratio, indicating that the coupling of oxidative phosphorylation is preserved in the mitochondria of adipose tissue with ageing (Kraunsoe *et al.* 2010; Larsen *et al.* 2012). However, although not different with only succinate, the lower substrate control ratios for octanoyl–carnitine alone and in combination with succinate are indicative of a reduced response to these substrates in the adipose tissue mitochondria of old mice. This reduction in the response to lipid substrates may contribute to an age-associated increase in mitochondrial ROS production (Turrens, 2003; Kraunsoe *et al.* 2010; Larsen *et al.* 2012) and the documented increase in nitrotyrosine abundance in the visceral WAT from old mice (Fig. 3). Interestingly, the differences between young and old adipose tissue are similar to those described for visceral and subcutaneous adipose tissue biopsies obtained from obese patients undergoing bariatric surgery (Kraunsoe *et al.* 2010). As the visceral adipose tissue is believed to play a more crucial role in metabolic homeostasis, Kraunsoe *et al.* (2010) suggested that the reduction in substrate control ratio observed in the visceral (omental) adipose tissue relative to the subcutaneous adipose tissue was indicative of mitochondrial dysfunction. The present study provides direct evidence for a defect in visceral (epididymal) adipose tissue mitochondrial function in the setting of age-associated systemic metabolic dysfunction, evidenced here by increased HOMA-IR% and increased area under the curve during a glucose tolerance test. Specifically, the current findings reveal a clear reduction in responsiveness to lipid substrates in the mitochondria of the visceral WAT with age.

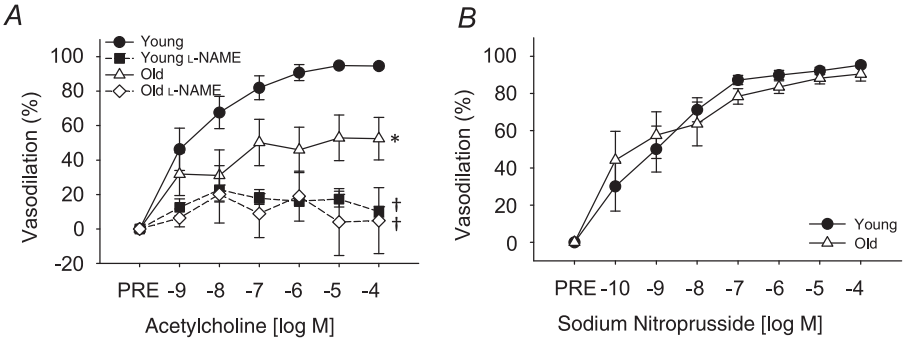

Figure 5. Endothelium-dependent dilation in eWAT resistance arteries from young and old mice
A, dose–responses to acetylcholine in the absence or presence of the nitric oxide synthase inhibitor, L-NAME, in eWAT resistance arteries from young ($n = 8$) and old ($n = 9$) mice. *B*, dose–responses to the endothelium independent vasodilator, sodium nitroprusside in eWAT resistance arteries from young ($n = 7$) and old ($n = 5$) mice. *Denotes group difference from young. †Denotes difference with L-NAME from acetylcholine alone. Differences in dose–responses were assessed by repeated measures ANOVA. Data are means ± S.E.M., $P \leq 0.05$. eWAT, epididymal white adipose tissue; L-NAME, N^G-nitro-L-arginine methyl ester.

Markers for brown adipose tissue have recently been demonstrated to be reduced within the subcutaneous, but not visceral, white adipose tissue with advancing age in C57Bl/6J mice (Rogers *et al.* 2012). In contrast to this previous report, here we find that 'beige' adipose tissue, assessed by measuring gene expression of the brown fat markers *Ucp1*, *Elovl3* and *Cidea1*, was reduced in the visceral WAT with age. Although the reason for these disparate findings between studies is unclear, strain specificity and animal age may be contributing factors. Nevertheless, reductions in beige adipose tissue within the visceral WAT observed in the present study may play a role in the apparent reduction in responsiveness to lipid substrates in the mitochondria of old mice (Festuccia *et al.* 2011) and to age-associated metabolic dysfunction in the old mice, including the tendency for both reduced daytime heat production and increased night-time respiratory exchange ratio, as well as the observed glucose intolerance (Table 2). Indeed, previous reports have revealed that *Ucp1* deletion results in metabolic dysfunction (Feldmann *et al.* 2009) and conversely, that high Ucp1 expression in the obese is associated with improved glucose tolerance (Timmons & Pedersen, 2009). Although an assessment of protein expression for these markers would be preferred, the low levels of expression of brown fat markers in the white adipose tissue make them difficult to assess by Western blot. However, measuring RNA as an assessment of changes in beige adipose tissue is an approach that has been used by other investigators previously (Rogers *et al.* 2012; Harms & Seale, 2013).

Angiogenesis, vascularity and ageing

Adipose tissue growth and adipocyte differentiation are dependent on the appropriate and co-ordinated development of the vascular system (Rupnick *et al.* 2002) and inadequate vascularity may contribute to tissue hypoxia, oxidative stress and inflammation that can lead to metabolic dysfunction (Gregor & Hotamisligil, 2007; Zhang *et al.* 2011; Yilmaz & Hotamisligil, 2013). Here, we found a reduced vascularity in the adipose tissue of older mice, a potential contributor to tissue hypoxia and reduced substrate delivery with ageing. VEGF is released from the endothelium in response to tissue hypoxia and induces neovessel formation in an attempt to normalize oxygen and nutrient delivery (Sun *et al.* 2011). However, in aged mice, *Vegf* expression was lower and there was a reduced capacity for angiogenic sprouting in our *in vitro* assay. Thus, it appears that an inadequate induction of *Vegf* and/or a reduced angiogenic potential in the adipose tissue of aged mice may contribute to tissue dysfunction.

Endothelium-dependent dilation and ageing

In young healthy animals at rest, the visceral adipose tissue receives a large proportion of cardiac output (~12%) and this is reduced by almost 50% with advancing age (Davis *et al.* 2013). This reduction in blood flow with ageing cannot be explained by an increase in vasoconstriction of the adipose arteries as both spontaneous tone and agonist elicited vasoconstriction are actually diminished in the resistance arteries of the adipose tissue from old rats that were cleared of the surrounding adipocytes (Davis *et al.* 2013). In the present study, we also found a small reduction in pre-constriction to phenylephrine in old compared to young mice, although this difference was not significant. Importantly, we further demonstrated that L-NAME resulted in a significant increase in pre-constriction in the young but not old mice, indicative of a reduced contribution of NO to basal artery diameter in the old mice and providing initial evidence for a defect in NO bioavailability in eWAT arteries with ageing.

Recently, we demonstrated that high fat diet impairs EDD and reduces the bioavailability of NO in the resistance arteries of adipose tissue that were cleared of the surrounding adipocytes from young mice (Donato *et al.* 2012) and that this endothelial dysfunction was associated with metabolic dysfunction and adipose tissue inflammation. Here, we demonstrate a similar decrease in EDD and reduced NO bioavailability in cleared adipose tissue arteries with advancing age. In a recent article (Meijer *et al.* 2013), the authors describe a reduction in insulin-mediated dilation in skeletal muscle arteries of obese mice that is mediated by adipose-derived c-Jun kinase-associated inflammatory signalling. A similar adipose-associated inflammatory mechanism may be an important contributor to *in vivo* decrements in adipose artery dilation in aged mice. The influence of the surrounding adipocyte on vascular function is an interesting and important question; however, as this was not the focus of the present study, we removed the surrounding adipocytes from all vessels to eliminate a potential confounding effect as well as to allow for proper visualization of the lumen that is required for pressure myography. Determining the impact of the surrounding adipocytes to vessel function is an important area for future investigation. Nevertheless, in the present study, we demonstrate a defect in EDD characterized by a reduction in NO bioavailability in the eWAT arteries of old mice that occurs even when the surrounding adipose is removed and this endothelial dysfunction probably has important functional implications on the tissue. NO is an important endothelium-derived molecule that not only induces relaxation of the vascular smooth muscle and consequently induces vasodilation (Ignarro *et al.* 1987), but also acts in concert with VEGF to promote angiogenesis (Cooke & Losordo, 2002). Thus, age-associated endothelial dysfunction in eWAT arteries may limit not only adipose tissue blood flow, but also the angiogenic capacity of the tissue, contributing to adipose dysfunction with advancing age.

Relevance to human ageing

Although, some humans gain body mass in older age (Newman *et al.* 2005), there is a large body of evidence that demonstrates humans (Baumgartner *et al.* 1995; Wallace *et al.* 1995; Kyle *et al.* 2001), rats (Yu *et al.* 1982) and mice (Yamate *et al.* 1990) increase in body mass until late middle age with a progressive loss in body mass observed thereafter (Williamson, 1993). Indeed, in a 10-year NHANES follow-up among older women stratified for BMI, nearly every BMI stratum lost weight over the 10-year period (66–76 years) (Launer *et al.* 1994). Importantly, the changes in body fat mass are similar to changes in total body mass in older adults (Newman *et al.* 2005). Indeed, although fat mass is known to increase with advancing age into middle-age and early old age, fat mass decreases into older age (Shimokata *et al.* 1989; Kirkland *et al.* 2002). In a 5-year longitudinal study of over 1900 normal weight (BMI ∼27) male and female subjects aged 70–79 years at baseline, there was a mean decrease in adipose volume, measured by CT, in both subcutaneous and visceral adipose tissue depots (Rossi *et al.* 2011). Similar reductions in fat mass were also found in older adults (>70–80 years) when subcutaneous fat was assessed by skin-fold measures (Chumlea *et al.* 1989; Ravaglia *et al.* 1999) or total fat mass was assessed by dual emission X-ray absorptiometry (Ravaglia *et al.* 1999).

The old mice in the present study are ∼30 months of age and this equates to a human age of ∼75–80 years. The lower epididymal adipose mass and reduced visceral and subcutaneous adipose tissue volumes in the old mice mirror that of the shifting adipose profile in the aged human population (Kirkland *et al.* 2002). Despite the loss of fat mass/volume, oxygen consumption was similar and food intake was higher in the old compared to young mice, suggesting that the loss of fat mass in the adipose depots of our old mice is not simply the consequence of frailty associated anorexia (Vanitallie, 2003). Rather, the loss of fat in the entopic depots may reflect a defect in lipid handling in the adipose with advanced age. Furthermore, the observed redistribution of stored lipids away from entopic towards ectopic storage sites is reminiscent of lipodystrophic conditions that, like advancing age, are associated with impaired glucose tolerance and insulin resistance. Thus, the B6D2F1 model appears to demonstrate most aspects of adipose tissue dysfunction, which may represent a good model for future investigations into the impact of ageing on the adipose tissue.

Conclusions and future directions

Age-associated metabolic dysfunction, i.e. glucose intolerance and increased HOMA-IR%, is accompanied by dysfunction of the adipose tissue and its associated vasculature. Our results indicate that advancing age is associated with a loss of adipocyte lipid storage capacity and increases in adipose tissue fibrosis and ectopic (hepatic) lipid storage. There is also a shift in the adipose tissue genotype such that aged WAT has a reduced expression of brown, or 'beige' adipose markers. We also found that the adipose tissue mitochondria have reduced responsiveness to lipids with age and that there is endothelial dysfunction in the arteries of aged adipose tissue, characterized by reduced vascularity, impaired angiogenesis and reduced vasodilation. Thus, metabolic dysfunction with advancing age occurs in concert with dysfunction in the adipose tissue. The present study also provides evidence that this adipose tissue, adipose artery and adipose mitochondrial dysfunction, are concomitant with metabolic dysfunction and occur even in the absence of the rapid, malnutrition-related rapid unexplained weight loss that is normally associated with the onset of frailty (Vanitallie, 2003). Future studies should be performed to elucidate if the arterial and mitochondrial defects are an underlying cause of the adipose and metabolic dysfunction and if therapeutics aimed at improving arterial or mitochondrial function in the adipose can improve/restore the lipid storage capacity of the entopic adipose depots and improve metabolic function. In addition, an examination of metabolic, adipose tissue, and adipose artery and mitochondrial function at multiple time points throughout the lifespan should be undertaken in future studies.

References

Baumgartner RN, Stauber PM, McHugh D, Koehler KM & Garry PJ (1995). Cross-sectional age differences in body composition in persons 60+ years of age. *J Gerontol A Biol Sci Med Sci* **50**, M307–M316.

Chumlea WC, Rhyne RL, Garry PJ & Hunt WC (1989). Changes in anthropometric indices of body composition with age in a healthy elderly population. *Am J Hum Biol* **1**, 457–462.

Cooke JP & Losordo DW (2002). Nitric oxide and angiogenesis. *Circulation* **105**, 2133–2135.

Cree MG, Newcomer BR, Katsanos CS, Sheffield-Moore M, Chinkes D, Aarsland A, Urban R & Wolfe RR (2004). Intramuscular and liver triglycerides are increased in the elderly. *J Clin Endocrinol Metab* **89**, 3864–3871.

Davis RT 3rd, Stabley JN, Dominguez JM 2nd, Ramsey MW, McCullough DJ, Lesniewski LA, Delp MD & Behnke BJ (2013). Differential effects of aging and exercise on intra-abdominal adipose arteriolar function and blood flow regulation. *J Appl Physiol* **114**, 808–815.

Divoux A, Tordjman J, Lacasa D, Veyrie N, Hugol D, Aissat A, Basdevant A, Guerre-Millo M, Poitou C, Zucker JD, Bedossa P & Clement K (2010). Fibrosis in human adipose tissue: composition, distribution, and link with lipid metabolism and fat mass loss. *Diabetes* **59**, 2817–2825.

Donato AJ, Henson GD, Morgan RG, Enz RA, Walker AE & Lesniewski LA (2012). TNF-alpha impairs endothelial function in adipose tissue resistance arteries of mice with diet-induced obesity. *Am J Physiol Heart Circ Physiol* **303**, H672–H679.

Eckel RH, Grundy SM & Zimmet PZ (2005). The metabolic syndrome. *Lancet* **365**, 1415–1428.

Feldmann HM, Golozoubova V, Cannon B & Nedergaard J (2009). UCP1 ablation induces obesity and abolishes diet-induced thermogenesis in mice exempt from thermal stress by living at thermoneutrality. *Cell Metab* **9**, 203–209.

Festuccia WT, Blanchard PG & Deshaies Y (2011). Control of brown adipose tissue glucose and lipid metabolism by PPARgamma. *Front Endocrinol (Lausanne)* **2**, 84.

Frayn KN (2002). Adipose tissue as a buffer for daily lipid flux. *Diabetologia* **45**, 1201–1210.

Garg A (2006). Adipose tissue dysfunction in obesity and lipodystrophy. *Clin Cornerstone* **8**(Suppl 4), S7–S13.

Gealekman O, Guseva N, Hartigan C, Apotheker S, Gorgoglione M, Gurav K, Tran KV, Straubhaar J, Nicoloro S, Czech MP, Thompson M, Perugini RA & Corvera S (2011). Depot-specific differences and insufficient subcutaneous adipose tissue angiogenesis in human obesity. *Circulation* **123**, 186–194.

Goodpaster BH, Carlson CL, Visser M, Kelley DE, Scherzinger A, Harris TB, Stamm E & Newman AB (2001). Attenuation of skeletal muscle and strength in the elderly: The Health ABC Study. *J Appl Physiol* **90**, 2157–2165.

Goossens GH (2008). The role of adipose tissue dysfunction in the pathogenesis of obesity-related insulin resistance. *Physiol Behav* **94**, 206–218.

Gregor MF & Hotamisligil GS (2007). Thematic review series: Adipocyte Biology. Adipocyte stress: the endoplasmic reticulum and metabolic disease. *J Lipid Res* **48**, 1905–1914.

Harms M & Seale P (2013). Brown and beige fat: development, function and therapeutic potential. *Nat Med* **19**, 1252–1263.

Ignarro LJ, Buga GM, Wood KS, Byrns RE & Chaudhuri G (1987). Endothelium-derived relaxing factor produced and released from artery and vein is nitric oxide. *Proc Natl Acad Sci U S A* **84**, 9265–9269.

Jackson RA, Hawa MI, Roshania RD, Sim BM, DiSilvio L & Jaspan JB (1988). Influence of aging on hepatic and peripheral glucose metabolism in humans. *Diabetes* **37**, 119–129.

Karakelides H, Irving BA, Short KR, O'Brien P & Nair KS (2010). Age, obesity, and sex effects on insulin sensitivity and skeletal muscle mitochondrial function. *Diabetes* **59**, 89–97.

Kelley DE, Goodpaster B, Wing RR & Simoneau JA (1999). Skeletal muscle fatty acid metabolism in association with insulin resistance, obesity, and weight loss. *Am J Physiol Endocrinol Metab* **277**, E1130–E1141.

Khan T, Muise ES, Iyengar P, Wang ZV, Chandalia M, Abate N, Zhang BB, Bonaldo P, Chua S & Scherer PE (2009). Metabolic dysregulation and adipose tissue fibrosis: role of collagen VI. *Mol Cell Biol* **29**, 1575–1591.

Kirkland JL & Dobson DE (1997). Preadipocyte function and aging: links between age-related changes in cell dynamics and altered fat tissue function. *J Am Geriatr Soc* **45**, 959–967.

Kirkland JL, Hollenberg CH, Kindler S & Gillon WS (1994). Effects of age and anatomic site on preadipocyte number in rat fat depots. *J Gerontol* **49**, B31–35.

Kirkland JL, Tchkonia T, Pirtskhalava T, Han J & Karagiannides I (2002). Adipogenesis and aging: does aging make fat go MAD? *Exp Gerontol* **37**, 757–767.

Koonen DP, Sung MM, Kao CK, Dolinsky VW, Koves TR, Ilkayeva O, Jacobs RL, Vance DE, Light PE, Muoio DM, Febbraio M & Dyck JR (2010). Alterations in skeletal muscle fatty acid handling predisposes middle-aged mice to diet-induced insulin resistance. *Diabetes* **59**, 1366–1375.

Kraunsoe R, Boushel R, Hansen CN, Schjerling P, Qvortrup K, Stockel M, Mikines KJ & Dela F (2010). Mitochondrial respiration in subcutaneous and visceral adipose tissue from patients with morbid obesity. *J Physiol* **588**, 2023–2032.

Kyle UG, Genton L, Hans D, Karsegard L, Slosman DO & Pichard C (2001). Age-related differences in fat-free mass, skeletal muscle, body cell mass and fat mass between 18 and 94 years. *Eur J Clin Nutr* **55**, 663–672.

Larsen S, Hey-Mogensen M, Rabol R, Stride N, Helge JW & Dela F (2012). The influence of age and aerobic fitness: effects on mitochondrial respiration in skeletal muscle. *Acta Physiol* **205**, 423–432.

Launer LJ, Harris T, Rumpel C & Madans J (1994). Body mass index, weight change, and risk of mobility disability in middle-aged and older women. The epidemiologic follow-up study of NHANES I. *JAMA* **271**, 1093–1098.

Lesniewski LA, Hosch SE, Neels JG, de Luca C, Pashmforoush M, Lumeng CN, Chiang SH, Scadeng M, Saltiel AR & Olefsky JM (2007). Bone marrow-specific Cap gene deletion protects against high-fat diet-induced insulin resistance. *Nat Med* **13**, 455–462.

Lesniewski LA, Connell ML, Durrant JR, Folian BJ, Anderson MC, Donato AJ & Seals DR (2009). B6D2F1 Mice are a suitable model of oxidative stress-mediated impaired endothelium-dependent dilation with aging. *J Gerontol A Biol Sci Med Sci* **64**, 9–20.

Levy JC, Matthews DR & Hermans MP (1998). Correct homeostasis model assessment (HOMA) evaluation uses the computer program. *Diabetes Care* **21**, 2191–2192.

Lindstrom J & Tuomilehto J (2003). The diabetes risk score: a practical tool to predict type 2 diabetes risk. *Diabetes Care* **26**, 725–731.

Lumeng CN, DelProposto JB, Westcott DJ & Saltiel AR (2008). Phenotypic switching of adipose tissue macrophages with obesity is generated by spatiotemporal differences in macrophage subtypes. *Diabetes* **57**, 3239–3246.

Mansouri A, Muller FL, Liu Y, Ng R, Faulkner J, Hamilton M, Richardson A, Huang TT, Epstein CJ & Van Remmen H (2006). Alterations in mitochondrial function, hydrogen peroxide release and oxidative damage in mouse hind-limb skeletal muscle during aging. *Mech Ageing Devt* **127**, 298–306.

Meijer RI, Bakker W, Alta CL, Sipkema P, Yudkin JS, Viollet B, Richter EA, Smulders YM, van Hinsbergh VW, Serne EH & Eringa EC (2013). Perivascular adipose tissue control of insulin-induced vasoreactivity in muscle is impaired in db/db mice. *Diabetes* **62**, 590–598.

National Research Council (U.S.). Committee for the Update of the Guide for the Care and Use of Laboratory Animals, Institute for Laboratory Animal Research (U.S.) & National Academies Press (U.S.). (2011). *Guide for the care and use of laboratory animals*. National Academies Press, Washington, D.C.

Newman AB, Lee JS, Visser M, Goodpaster BH, Kritchevsky SB, Tylavsky FA, Nevitt M & Harris TB (2005). Weight change and the conservation of lean mass in old age: the Health, Aging and Body Composition Study. *Am J Clin Nutr* **82**, 872–878; quiz 915–876.

Ravaglia G, Forti P, Maioli F, Boschi F, Cicognani A & Gasbarrini G (1999). Measurement of body fat in healthy elderly men: a comparison of methods. *J Gerontol A Biol Sci Med Sci* **54**, M70–M76.

Reddy AK, Li YH, Pham TT, Ochoa LN, Trevino MT, Hartley CJ, Michael LH, Entman ML & Taffet GE (2003). Measurement of aortic input impedance in mice: effects of age on aortic stiffness. *Am J Physiol Heart Circ Physiol* **285**, H1464–H1470.

Rodriguez-Sureda V & Peinado-Onsurbe J (2005). A procedure for measuring triacylglyceride and cholesterol content using a small amount of tissue. *Anal Biochem* **343**, 277–282.

Rogers NH, Landa A, Park S & Smith RG (2012). Aging leads to a programmed loss of brown adipocytes in murine subcutaneous white adipose tissue. *Aging Cell* **11**, 1074–1083.

Rossi AP, Watson NL, Newman AB, Harris TB, Kritchevsky SB, Bauer DC, Satterfield S, Goodpaster BH & Zamboni M (2011). Effects of body composition and adipose tissue distribution on respiratory function in elderly men and women: the health, aging, and body composition study. *J Gerontol A Biol Sci Med Sci* **66**, 801–808.

Rupnick MA, Panigrahy D, Zhang CY, Dallabrida SM, Lowell BB, Langer R & Folkman MJ (2002). Adipose tissue mass can be regulated through the vasculature. *Proc Natl Acad Sci U S A* **99**, 10730–10735.

Shimokata H, Tobin JD, Muller DC, Elahi D, Coon PJ & Andres R (1989). Studies in the distribution of body fat: I. Effects of age, sex, and obesity. *J Gerontol* **44**, M66–M73.

Sun K, Kusminski CM & Scherer PE (2011). Adipose tissue remodeling and obesity. *J Clin Invest* **121**, 2094–2101.

Timmons JA & Pedersen BK (2009). The importance of brown adipose tissue. *N Engl J Med* **361**, 415–416; author reply 418–421.

Trayhurn P & Wood IS (2004). Adipokines: inflammation and the pleiotropic role of white adipose tissue. *Br J Nutr* **92**, 347–355.

Turner RC, Holman RR, Matthews D, Hockaday TD & Peto J (1979). Insulin deficiency and insulin resistance interaction in diabetes: estimation of their relative contribution by feedback analysis from basal plasma insulin and glucose concentrations. *Metabolism* **28**, 1086–1096.

Turrens JF (2003). Mitochondrial formation of reactive oxygen species. *J Physiol* **552**, 335–344.

Vanitallie TB (2003). Frailty in the elderly: contributions of sarcopenia and visceral protein depletion. *Metabolism* **52**, 22–26.

Wallace JI, Schwartz RS, LaCroix AZ, Uhlmann RF & Pearlman RA (1995). Involuntary weight loss in older outpatients: incidence and clinical significance. *J Am Geriatr Soc* **43**, 329–337.

Williamson DF (1993). Descriptive epidemiology of body weight and weight change in U.S. adults. *Ann Intern Med* **119**, 646–649.

Wu D, Ren Z, Pae M, Guo W, Cui X, Merrill AH & Meydani SN (2007). Aging up-regulates expression of inflammatory mediators in mouse adipose tissue. *J Immunol* **179**, 4829–4839.

Yamate J, Tajima M, Kudow S & Sannai S (1990). Background pathology in BDF1 mice allowed to live out their life-span. *Lab Anim* **24**, 332–340.

Yilmaz M & Hotamisligil GS (2013). Damned if you do, damned if you don't: the conundrum of adipose tissue vascularization. *Cell Metab* **17**, 7–9.

Yu BP, Masoro EJ, Murata I, Bertrand HA & Lynd FT (1982). Life span study of SPF Fischer 344 male rats fed ad libitum or restricted diets: longevity, growth, lean body mass and disease. *J Gerontol* **37**, 130–141.

Zhang L, Ebenezer PJ, Dasuri K, Fernandez-Kim SO, Francis J, Mariappan N, Gao Z, Ye J, Bruce-Keller AJ & Keller JN (2011). Aging is associated with hypoxia and oxidative stress in adipose tissue: implications for adipose function. *Am J Physiol Endocrinol Metab* **301**, E599–E607.

Additional Information

Competing interests

None.

Author contributions

L.A.L. and A.J.D. contributed to all aspects of the study, including the conception and design of the experiments, collection, analyses, interpretation of data, and drafting and revision of the manuscript. G.D.H., C.R.H., G.L., J.D.T., K.D.R., R.C.B., R.G.M., R.A.E., S.H., A.E.W. and R.S.R. contributed to the collection and analysis of data and revision of the manuscript. All authors have read and approved the final submission of this article. All experiments were performed in the Translational Vascular Physiology (TVP) and the Utah Vascular Research (UVR) Laboratories at the University of Utah and VAMC-SLC GRECC.

Funding

This work was supported by awards from the National Institute on Aging and the National Heart Lung and Blood Institute; K01 AG033196, R21 AG033755, T35HL007744, R01 AG040297, P01 HL091830 and T32 HL007576, R21 AG043952 and VA Merit E6910R.